

Analysis of square and rectangular footings subjected to eccentric-inclined load resting on reinforced sand

Swami Saran · Surendra Kumar · K.G. Garg · Arvind Kumar

Received: 6 March 2006 / Accepted: 24 April 2006 / Published online: 29 September 2006
© Springer Science+Business Media B.V. 2006

Abstract In the present paper, a method of analysis for calculating the pressure intensity corresponding to a given settlement for eccentrically and obliquely loaded square and rectangular footings resting on reinforced soil foundation has been presented. The process has been simplified by presenting non-dimensional charts for the various terms used in the analysis, which can be directly used by practicing engineers. An approximate method has been suggested to find out the ultimate bearing capacity of such footings on reinforced soil. The results have been validated with the model test results. The procedure has been made clear by giving an illustrative example.

Keywords Eccentrically and obliquely loaded footings · Reinforced soil foundations · Non dimensional charts

S. Saran
Department of Civil Engineering, Indian Institute of Technology, Roorkee, India

S. Kumar · K. G. Garg
Geotechnical Engineering Division, CBRI, Roorkee, India

A. Kumar (✉)
Department of Civil Engineering, National Institute of Technology, Jalandhar, Punjab 144011, India
e-mail: agnihotriak@nitj.ac.in

Symbols

B	width of footing
D_R	depth of bottom most reinforcement layer
e	eccentricity
f	soil reinforcement frictional coefficient
Φ_r	soil – reinforcement friction angle
γ	unit weight of sand
i	load inclination
I_{xz}	dimensionless normal shear force component for computation of driving force of reinforcing layer at depth z
J_{xz}	dimensionless vertical normal force component in x direction for computation of driving force of reinforcing layer at depth z
J_{yz}	dimensionless vertical normal force component in y direction for computation of driving force of reinforcing layer at depth z
L_r	length of reinforcing layer
LDR	linear density of reinforcement
M_{xz}	dimensionless normal force component in x -direction for computation of soil-reinforcement frictional resistance of reinforcing layer at depth Z .
M_{yz}	dimensionless normal force component in y -direction for computation of soil-reinforcement frictional resistance of reinforcing layer at depth Z .
q_{ur}	ultimate bearing capacity of reinforced sand

N_q	Terzaghi's bearing capacity factor
T_R	allowable tensile strength of reinforcement per unit length
T_f	reinforcement pullout frictional resistance
T_D	driving force in reinforcement

Introduction

Soil is poor in its mechanical properties, in spite of this fact; it is used as the readily available construction material. It is also well established that the granular soils are strong in compression and shear but weak in tension. However, the strength of weak granular (e.g. loose and medium dense sand) materials can substantially be improved by introducing the reinforcing elements, like geogrids, geotextiles etc., within the significant zone of influence with a suitable layout arrangement and configuration. The beneficial effects of using tensile reinforcement to increase the bearing capacity of soil have been clearly demonstrated by several investigators (Binquet and Lee 1975a, b; Akinmusuru and Akinbolade 1981; Das and Larbi-Cherif 1983; Fragaszy and Lawton 1984; Guido et al. 1986; Huang and Tatsuoka 1990; Dixit and Mandal 1993; Khing et al. 1993; 1994; Murthy et al. 1993; Omar et al. 1993a, b; 1994; Yetimoglu et al. 1994; Adams and Collin 1997; Yoo 2001; Kumar and Saran 2001; 2003a, b, c; 2004; Kumar et al. 2005).

For designing foundations subjected to earthquake forces, adopting appropriate values of horizontal and vertical seismic coefficients, equivalent seismic forces can be conveniently evaluated. These forces in combination with static forces make the foundations subjected to eccentric inclined loads.

The aim of analysis proposed in this paper is an attempt to obtain the pressure intensity of strip footing on reinforced soil, for a known settlement (S) and pressure intensity (q_0) of the same footing resting on unreinforced sand.

The theoretical analyses proposed by Binquet and Lee (1975a, b) to compute the pressure intensity of strip footing which was extended by Kumar (1997) and Kumar and Saran (2003a, b, c)

for central vertical loading has been further extended to compute the pressure intensity for the square and rectangular footings subjected to eccentric-inclined load, resting on reinforced soil, for the known settlement of the same footing resting on unreinforced soil and subjected to the similar loading conditions.

It is the prerequisite that the aforementioned analyses require the value of pressure intensity, at a given settlement, of footings on unreinforced soil subjected to the similar type of loading. For footings subjected to eccentric-inclined loads, pressure-settlement curves can be obtained by the analysis proposed by Agrawal (1986) and Saran and Agrawal (1991) using the constitutive relations of the soil.

Pressure ratio, p_r

In order to express and compare the data a term, pressure ratio, has been conveniently introduced, which is defined as:

$$p_r = q/q_0 \quad (1)$$

where q_0 = the average contact pressure of footing on unreinforced sand at settlement, S . q = the average contact pressure of footing on reinforced sand at the same settlement, i.e., S

Assumptions

1. As the footing load increases, the footing and soil beneath moves downward, while the soil to the sides moves outward. The boundary between the downward moving and the outward moving zones has been assumed as the locus of points of maximum shear stress at every depth z .
2. At the surface separating the downward moving and outward zones, the reinforcement has been assumed to undergo two right angle bends around two frictionless rollers and the reinforcement resistance is a vertically acting tensile force.
3. The soil-reinforcement friction coefficient has been assumed to vary with depth in accordance with the following equation:

$$f_e = mf \tag{2}$$

where f = coefficient of friction between soil and reinforcement, m = mobilisation factor given by

$$m = (1 - z/B)0.7 + 0.3 \quad \text{for } z/B \leq 1.0$$

$$= (2 - z/B)0.3 \quad \text{for } z/B > 1.0$$

4. The driving force in reinforcement on different layer of reinforcement has been assumed to vary in proportion of $r_1: r_2: r_3 \dots r_i$, such that $r_1+r_2+r_3+\dots+r_i=1$. The failure mechanism has been assumed for various combinations of the reinforcement pullout and reinforcement breakage at different levels.
5. Forces calculated in the analyses are for the same footing size and shape, subjected to the same loading condition, at a given settlement, for footing on reinforced and unreinforced soil.
6. Normal and shear stresses inside the soil mass have been obtained using equations of the theory of elasticity.

Analysis

Consider a rectangular footing of width ‘ B ’ and length ‘ L ’ subjected to eccentric-inclined load of

intensity q (P/A). The normal and shear stresses at any point (x, y, z) in the soil mass, required for the calculation of the driving force and pull-out frictional resistance, have been computed by using the theory of elasticity (Poulos and Davis 1974).

Evaluation of driving force in reinforcement, T_D

Shear stress distribution at various depths z in the x and y -directions is shown in Fig. 1. Let X_0, X_1 and X_2 be the horizontal positions, along x -axis, of zero shear stress, maximum shear stress (τ_{xz}) to the side of the eccentricity and the maximum shear stress to the opposite side of the eccentricity, respectively, as shown in Figs. 2 and 3. Also, let Y_0 define the horizontal positions, along the y -axis, of the maximum shear stress (τ_{yz}), as shown in Figs. 2 and 3. However, the distribution of the stress along the y -axis is symmetrical about the x -axis since the load has only x -axis eccentricity. The extent of X_0, X_1 and X_2 varies with the change in the eccentricity and inclination of the load and the depth beneath the footing.

The loci of points of maximum shear stress, which are equally the planes separating the downward and outward moving zones, at every

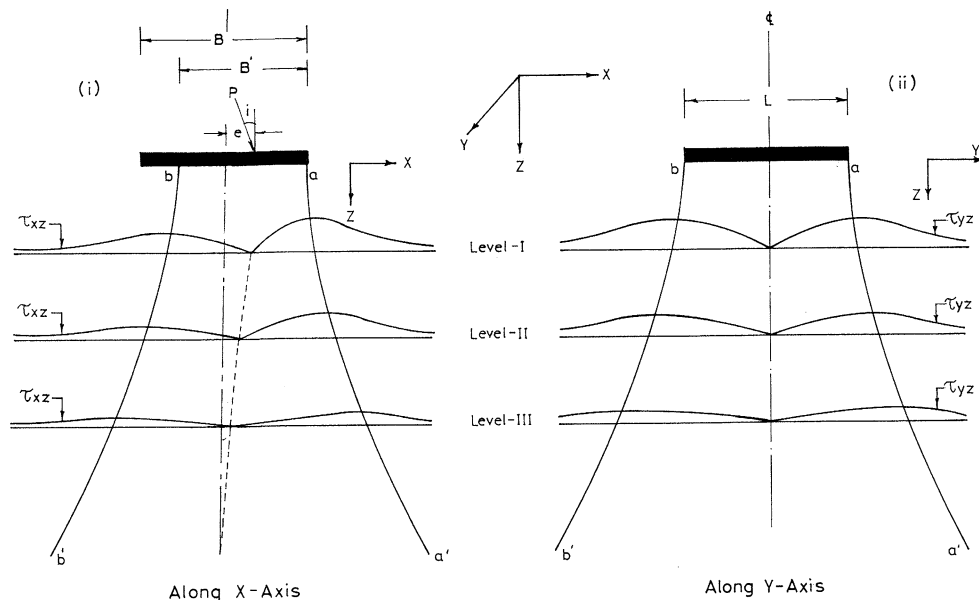


Fig. 1 Distribution of shear stresses beneath a rectangular footing subjected to eccentric inclined load

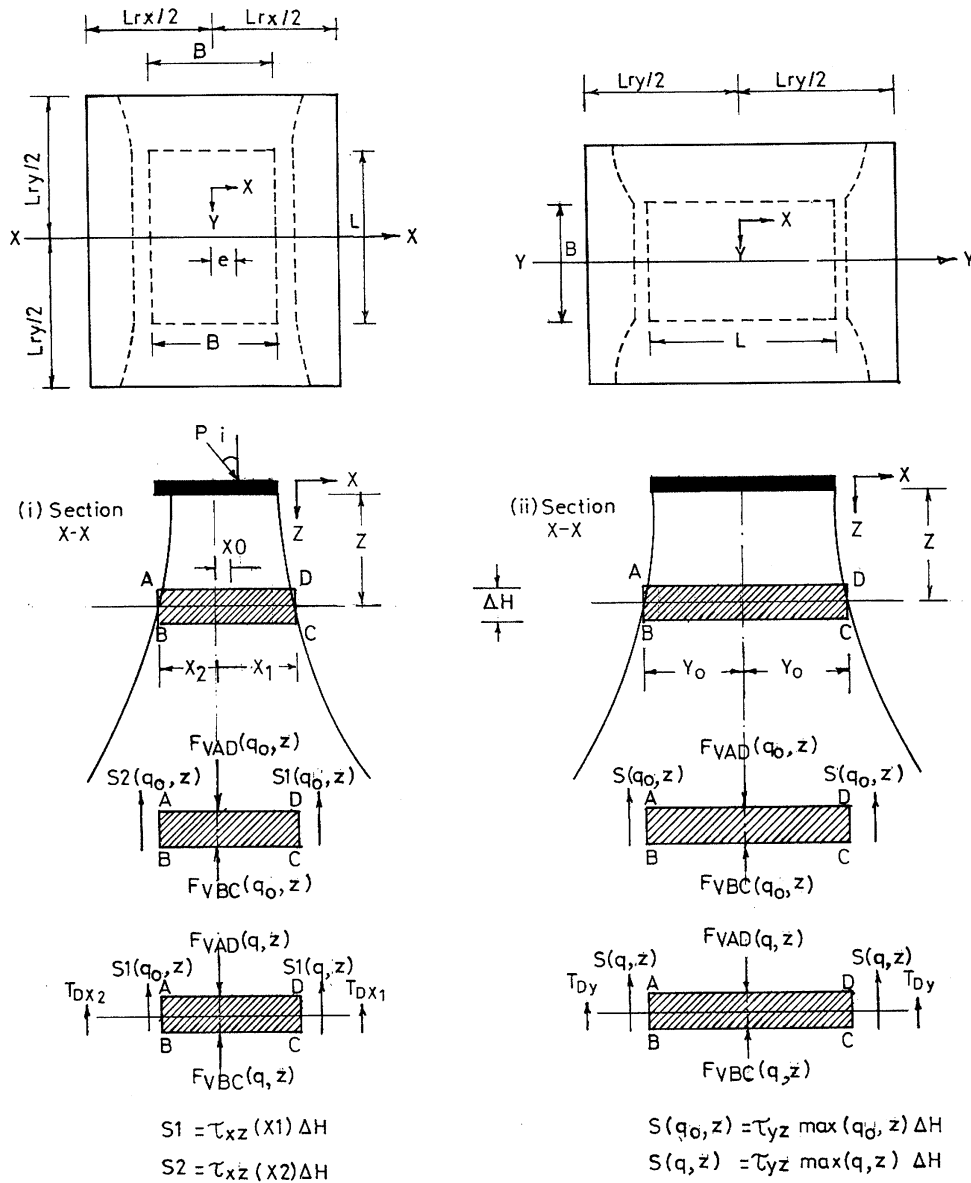


Fig. 2 Assumed separating planes and components of forces for pressure ratio calculation of rectangular footing subjected to eccentric inclined load on reinforced soil

depth z in the x and y -directions are shown in Fig. 2.

Consider an element $ABCD$ at depth z , as shown in Fig. 2 in the x -direction, which is the volume of soil inside the downward moving zone lying between two vertically adjacent layers of reinforcement. The forces acting on this element are shown in Fig. 2, for the cases of unreinforced and reinforced soil. The driving force will be in

both the x and y -directions, since the reinforcement is provided in these directions. Considering the equilibrium of all such elements along the whole length of the reinforcement at depth at z , Kumar (1997) and Kumar and Saran (2003a, b, c) developed the following expression for rectangular footing on reinforced sand, subjected to central vertical downward load, for one layer of reinforcement, along the x -direction:

$$T_{DX} = [J_{xz}BL - I_{xz}L\Delta H]q_0(p_r - 1) \tag{3}$$

But, for footings subjected to eccentric-inclined load, various terms in Eq. 3 are defined as follows:

$$T_{DX} = T_{DX1} + T_{DX2} \tag{4}$$

$$I_{xz} = I_{xz1} + I_{xz2} \tag{5}$$

where

$$I_{xz1} = \frac{1}{qL} \sum_{i=1}^{i=n} \tau_{xz} \left(\frac{X_{1i}}{B}, \frac{z}{B} \right) \partial y \tag{6}$$

$$I_{xz2} = \frac{1}{qL} \sum_{i=1}^{i=n} \tau_{xz} \left(\frac{X_{2i}}{B}, \frac{z}{B} \right) \partial y \tag{7}$$

$$I_{xz} = \frac{1}{qBL} \sum_{i=1}^{i=n} \int_{x=-X_2}^{x=X_1} \sigma_z dx \partial y \tag{8}$$

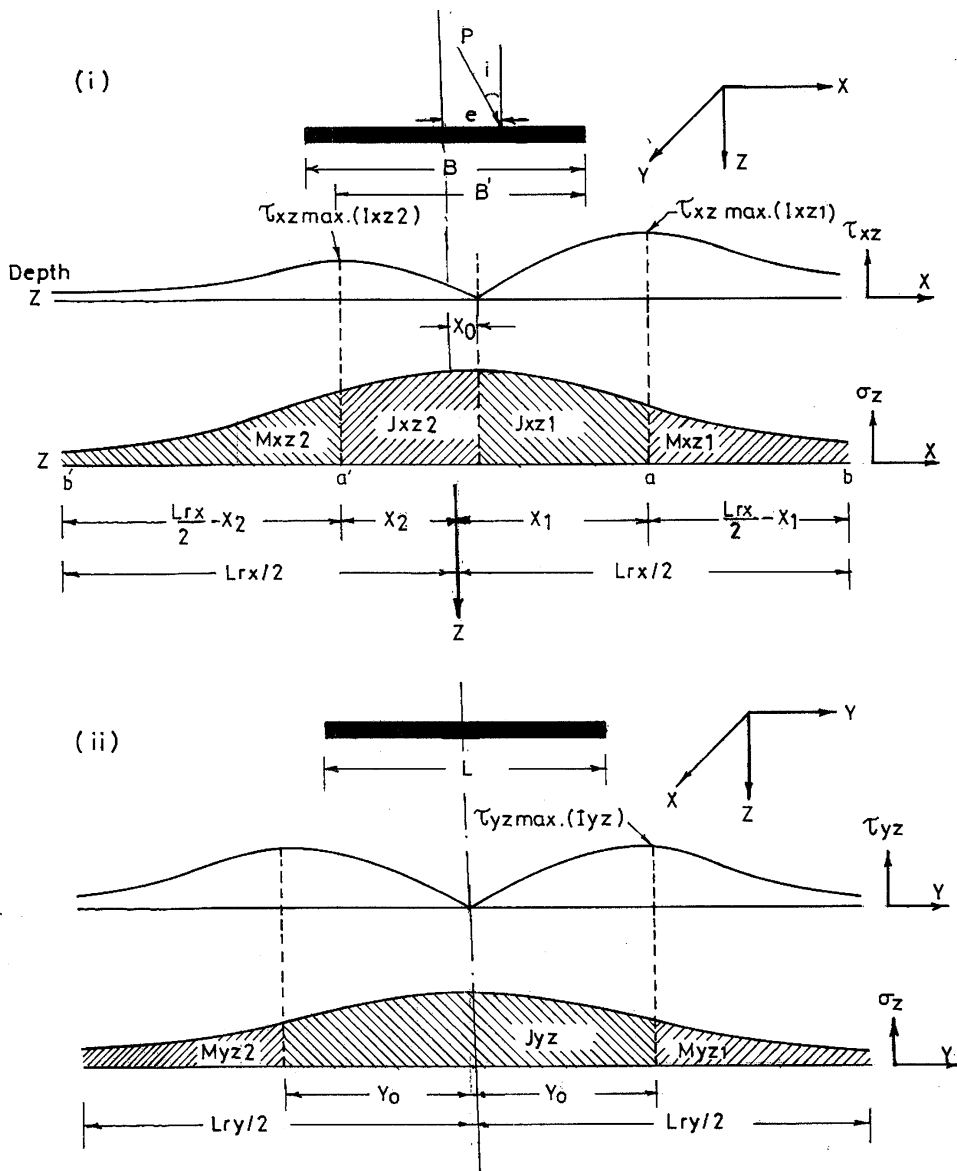


Fig. 3 Diagrams showing shear and normal stresses and non-dimensional forces in different directions

where X_{1i} and X_{2i} = the horizontal positions of shear stress peak at i th element, as shown in Figs. 2 and 3. L_{ry} = length of reinforcing layer in y -direction, ΔH = thickness of element, τ_{xz} and σ_z are the shear and normal stresses in the x -direction as shown in Figs. 2 and 3.

The interval $(X_{1i}+X_{2i})$ is divided into small units of size $0.01B$. The length reinforcing layer L_{ry} is divided into n intervals each of width $\partial y = 0.01B$.

Similarly, the developed tie force in the y -direction is given by:

$$T_{Dy} = [J_{yz}BL - I_{yz}B\Delta H]q_0(p_{r-1}) \tag{9}$$

which

$$I_{yz} = \frac{1}{qB} \sum_{i=1}^{i=n} \tau_{yz} \left(\frac{Y_{0i}}{B}, \frac{z}{B} \right) \partial x \tag{10}$$

$$J_{yz} = \frac{1}{qBL} \sum_{i=1}^{i=n} \int_{-Y_{0i}}^{Y_{0i}} \sigma_z dy \partial x \tag{11}$$

where Y_{0i} = position of maximum shear stress of i th element in y -direction L_{rx} = length of reinforcement layer in x -direction τ_{xz} and σ_z are the shear and normal stresses in the y -directions as shown in Fig. 3.

Equations 10 and 11 are solved by numerical integration. The value of Y_{0i} is divided into small units of value $0.01B$. The length of reinforcement L_{rx} is divided into n intervals each of width $\partial x=0.01B$.

The total driving force, T_D is given by:

$$T_D = T_{Dx} + T_{Dy} \tag{12}$$

Evaluation of pullout frictional resistance, T_f

The tie pullout frictional resistance will be due to the total normal force on the plan area of the reinforcement lying outside the assumed boundary separating the downward and outward moving zones, as shown in Figs. 2 and 3. The normal force, however, consists of two components, one is due to the applied bearing pressure and the other is

due to the normal overburden pressure of the soil. Considering both components over the whole area of reinforcement outside the separating plane, Kumar (1997) developed the following expression for rectangular footing subjected to central vertical downward load along the x -axis.

$$T_{fx} = 2f_e LDR [M_{xz}BLq_0p_r + yA_{xz}(z + D_f)BL] \tag{13}$$

For rectangular footing subjected to eccentric-inclined load the different terms of Eq. 12 will be as:

$$T_{fx} = T_{fx1} + T_{fx2} \tag{14}$$

$$M_{xz} = M_{xz1} + M_{xz2} \tag{15}$$

$$A_{xz} = A_{xz1} + A_{xz2} \tag{16}$$

$$M_{xz1} = \frac{1}{qBL} \sum_{i=1}^{i=n} \int_{x1}^{Lrx/2} \sigma_z dx \partial y \tag{17}$$

$$M_{xz2} = \frac{1}{qBL} \sum_{i=1}^{i=n} \int_{x2}^{Lry/2} \sigma_z dx \partial y \tag{18}$$

$$A_{xz1} = \frac{1}{BL} \sum_{i=1}^{i=n} \left(\frac{L_{rx}}{2} - X_{1i} \right) \partial y \tag{19}$$

$$A_{xz1} = \frac{1}{BL} \sum_{i=1}^{i=n} \left(\frac{L_{rx}}{2} - X_{2i} \right) \partial y \tag{20}$$

The above equations have been solved by numerical integration. The interval $(L_{rx}/2-X_{1i})$ and $(L_{rx}/2-X_{2i})$ is divided into small units of value $0.01B$. The width of reinforcement L_{rx} is divided into n intervals each of $0.01B$.

Where γ = unit weight of soil, D_f = embedment depth of footing

$$\begin{aligned} LDR &= \text{plan area of reinforcement/total} \\ &\quad \text{area of reinforced soil layer} \\ &= 1 \text{ for geogrid} \end{aligned}$$

f_e as given by Eq. 2

Similarly, the soil-reinforcement pullout frictional resistance in y -direction is expressed as follows:

$$T_{fy} = 2f_c LDR [M_{yz} BL q_0 p_r + \gamma A_{yz} (z + D_f) BL] \tag{21}$$

where

$$T_{fy} = T_{fy1} + T_{fy2} \tag{22}$$

$$M_{yz} = M_{yz1} + M_{yz2} \tag{23}$$

$$A_{yz} = A_{yz1} + A_{yz2} \tag{24}$$

$$M_{yz1} = M_{yz2} = \frac{1}{qBL} \sum_{i=1}^{i=n} \int_{Y_0}^{Lry/2} \sigma_z dy \partial x \tag{25}$$

$$A_{yz1} = A_{yz2} = \frac{1}{BL} \sum_{i=1}^n \left(\frac{Lry}{2} - Y_{0i} \right) \partial x \tag{26}$$

The above equations have been solved by numerical integration. The interval $(L_{rx}/2 - Y_{0i})$ is divided into small units of value $0.01B$. The width of reinforcement L_{rx} is divided into n intervals each of width $0.01B$.

Therefore the total tie pullout frictional resistance is given by

$$T_f = T_{fx} + T_{fy} \tag{27}$$

Numerical integration has been used to solve the above equations.

For square footing, the expressions of different parameters obtained for rectangular footing will be modified by applying the following substitutions: $L=B$ and $L_{rx}=L_{ry}=L_r$.

Non-dimensional chart for J_{xz} , J_{yz} , I_{xz} , I_{yz} , M_{xz} , M_{yz} , A_{xz} and A_{yz} at different layer levels, $z/B=0.25, 0.50, 0.75, 1.00, 1.25, 1.50, 1.75$ and 2.00 for square footing subjected to eccentric-inclined load have been prepared and presented elsewhere (Kumar 2002) in terms of eccentricity ratio ' e/B ', load inclination ' i ' and the size of reinforcing layers ' L/B in both x and y directions. Similarly the charts for rectangular footings ($L/B = 2, 3$ and 4) for different variables, as for square footings, have been prepared and are presented elsewhere

(Kumar 2002). Few typical charts are shown in Figs. 4 and 5.

Determination of pressure ratio (p_r)

The pressure ratio p_r has been computed by applying the following conditions:

- (1) The driving force in any layer should not exceed the reinforcement pullout frictional resistance, in the same layer i.e., $r_i T_{Di} \leq T_{fi}$ where, $i = 1, 2, \dots, N$
- (2) The driving force, in any layer, should not exceed the tie breaking strength of the same layer i.e., $r_i T_{Di} \leq T_{RF}$ where, T_{RF} = the total breaking force in that layer i.e. $T_{RF} = T_R \times$ length of reinforcement along which breaking may take place where T_R = allowable tensile strength of reinforcement per unit length M_i 's = distribution factors assumed for the distribution of the driving force in N -layers, such that $r_1 + r_2 + \dots + r_N = 1$

The check is applied for different combinations of reinforcement pullout and breaking failures. The maximum value shall be the critical p_r .

Ultimate bearing capacity of footing on reinforced sand

The analysis developed above is for computing the pressure intensity of square and rectangular footings on reinforced soil, as indicated earlier, for a given settlement (S), corresponding to pressure intensity (q_0) of the same footing, resting on unreinforced sand, at the same settlement (S). The pressure-settlement values of footings on reinforced sand, however, can only be computed, up to the ultimate bearing capacity of the unreinforced soil. Consequently, one of the limitations of the proposed analysis is that, the ultimate bearing capacity of footings on reinforced soil cannot be obtained directly.

Kumar (1997), Kumar and Saran (2003b) and Al-Smadi (1998) proposed an empirical approach for computing the ultimate bearing capacity of footings on reinforced soil by

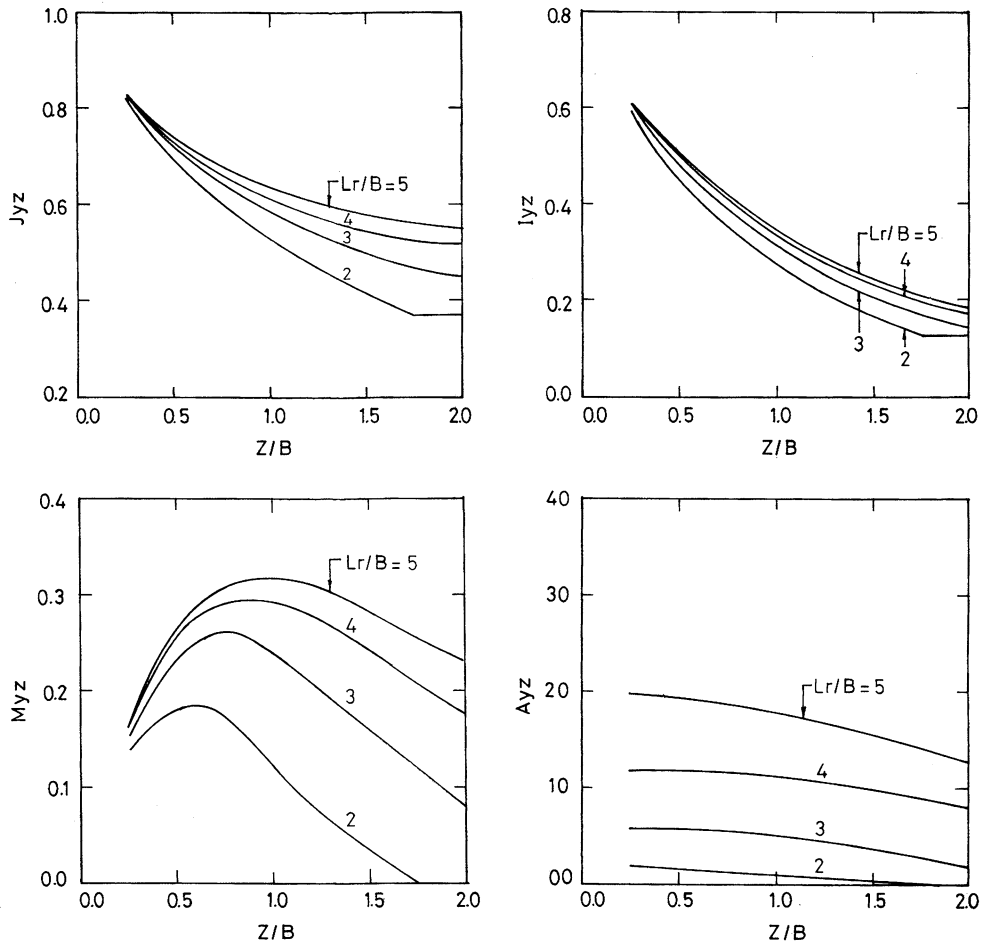


Fig. 4 Non-dimensional area and force components for computing pressure ratio of square footing on reinforced soil for $e/B = 0.1$ and $i = 10^\circ$ (X-direction)

extending the work of Singh (1988) and Huang and Tatsuoka (1990). Therefore, similar empirical approach, based on the model test results, has been introduced herein. As can be seen from Fig. 6 that

$$q_{ur} = q_r + \Delta q R_{iq} R_{eq} \tag{28}$$

where

$$\Delta q = \gamma D_f N_q \tag{29}$$

It has been observed that, the above Eqs. (24) and (25) hold good as long as the inclination i is less than or equal to 10° . However, when $i > 10^\circ$, Then

$$q_{ur} = q_r \tag{30}$$

where

$$R_{eq} = (1 - 2e/B)$$

$$R_q = (1 - i/90)^2$$

Reduction factors due to e/B and i
 = Load inclination in degrees

$D_f = D_R$ = depth of bottom most reinforcement layer; γ = unit weight of sand; N_q = Terzaghi's bearing capacity factor; q_{ur} = ultimate bearing capacity of reinforced sand; q_r = pressure intensity of footing on reinforced sand at settlement S_u corresponding to q_u of unreinforced sand.

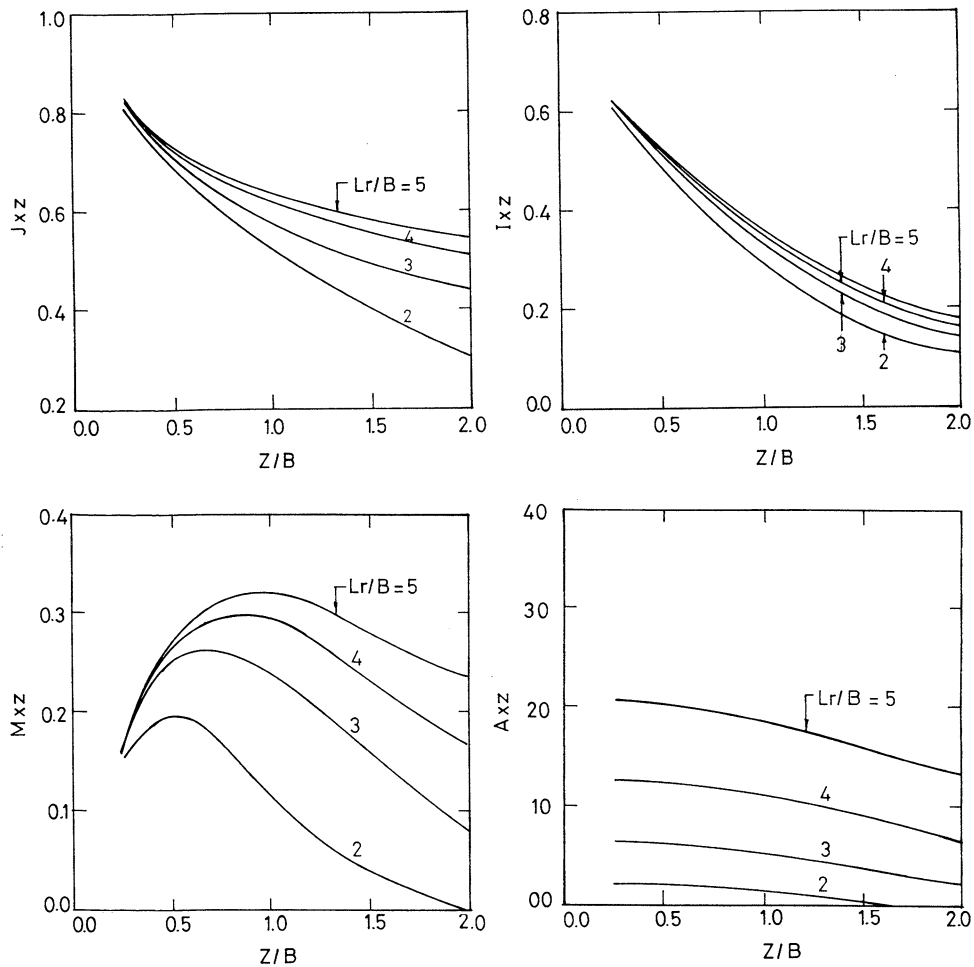


Fig. 5 Non-dimensional area and force components for computing pressure ratio of square footing on reinforced soil for $e/b = 0.1$ and $i = 10^\circ$ (Y-direction)

It has been observed that the aforementioned approach holds good if the value of D_R is less than or equal to footing width (B).

Experimental validation

Analysis, described above, has been verified for square footing for all the cases under consideration, namely:

- (1) $e/B = 0.0, 0.1$; $i = 0^\circ, 10^\circ$; $L_r/B = 1, 2, 3$ and $N = 1, 2, 3, 4$
- (2) $e/B = 0.0, 0.1$; $i = 20^\circ$; $L_r/B = 1, 2, 3$ and $N = 4$
- (3) $e/B = 0.2, i = 0^\circ, 10^\circ, 20^\circ$; $L_r/B = 1, 2, 3$ and $N = 4$

The procedure described above was followed for predicting the pressure ratio (p_r) and pressure intensity (q) of reinforced footing corresponding to the pressure intensity (q_0) of unreinforced footing at the same settlement. It has been observed experimentally that each layer of reinforcement failed in friction. When the footing is subjected to eccentric-inclined load the friction acting on the two sides of the footing; ab and $a'b'$ (Fig. 3) will be of different magnitude. It is very likely that full friction will be mobilized on the one side of the eccentric-inclined load and there will be only partial mobilization on the other side, it is not possible to quantify exactly the amount of mobilization of friction on this side. Keeping this in view a simple procedure was adopted in which

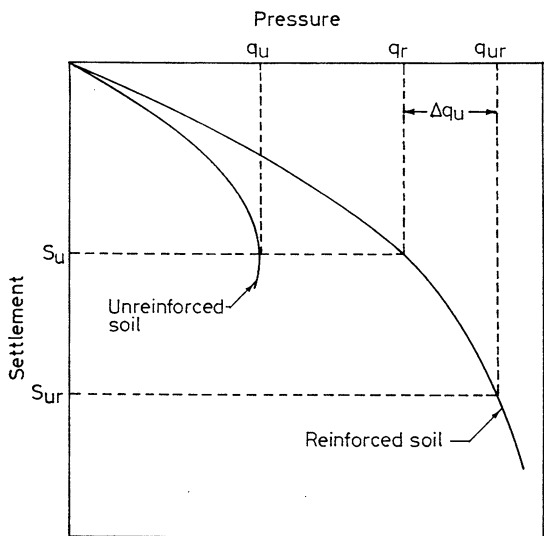


Fig. 6 Typical pressure versus settlement curves for a footing on unreinforced and reinforced soil

the full friction of both the side was estimated first and then multiplied by the reduction factors (Fig. 7) due to eccentricity (R_{fe}) and inclination (R_{fi}) are given in the Eqs. 30 and 31.

$$R_{fe} = 1 - 2e/B \tag{31}$$

$$R_{fi} = 1 - i/\Phi \tag{32}$$

A few typical samples of the observed and predicted pressure versus settlement (S_e) for square footings are shown in Fig. 8. It can be seen from the figures that the predicted results are in good agreement with the observed ones.

Similarly, the observed settlement versus predicted settlement curves are prepared for all the cases and are presented in Fig. 9. It can be seen from these figures that there is a good match between observed and predicted values of settlement.

Fig. 10 shows the observed (model tests) and predicted values of ultimate bearing capacity. And they are matching very well.

Design example

Statement

It is required to design a square footing resting on reinforced sand to carry safely, a central vertical

load ' P_v ' of 1200 kN, a horizontal shear load p_h of 210 kN and a moment ' M ' of 240 kN.m. The density of sand is 15 kN/m^3 and angle of internal friction is 35° . The pressure-settlement curve on unreinforced sand is given in Fig. 11. The sand below the footing is reinforced with geogrid of 20 kN/m strength and sand-geogrid frictional angle ϕ_f is 22° .

Solution

- (i) Taking a footing of width $B = 2000 \text{ mm}$, placed at a depth $D_f = 1000 \text{ mm}$ below the ground level.
- (ii) Eccentricity = $e = M/P_v = 240/1200 = 0.2 \text{ m}$
- (iii) Eccentric-inclined load P is given by

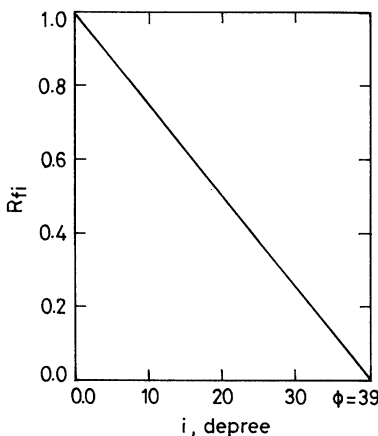
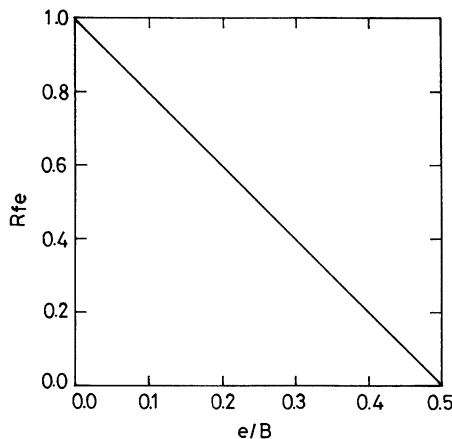


Fig. 7 Reduction factors due to eccentricity and inclination of the applied load considered for frictional force computation in reinforcement

$$P = \sqrt{P_v^2 + P_h^2} = \sqrt{1200^2 + 210^2} = 1218.2\text{kN}$$

$$P \approx 1220\text{kN}$$

(iv) Inclination of load from vertical

$$i = \tan^{-1}(P_h/P_v) = \tan^{-1}(210/1200)$$

$$= \tan^{-1}(0.175) = 9.93$$

$$\approx 10$$

(v) The ultimate load of a square footing subjected to eccentric-inclined load is given as:

$$Q_u = q_u A = [0.4\gamma B N_\gamma R_{e\gamma} R_{i\gamma} + \gamma D_f N_q R_{eq} R_{iq}] A$$

$$\gamma = 15.00\text{kN/m}^3, B = 1.0\text{m}, D_f = 1.0\text{m},$$

$$N_\gamma = 42.2 \ \& \ N_q = 40.0$$

$$R_{e\gamma} = 0.64, R_{i\gamma} = 0.51, R_{eq} = 0.80, R_{iq} = 0.79,$$

$$A = 2 \times 2 = 4\text{m}^2$$

$$Q_u = [(0.3264 \times 506.4) + (0.632 \times 600.0)] 4.0$$

$$= [165.29 + 379.20] 4.0 = 544.5 \times 4$$

$$= 2177.96 \approx 2178\text{kN}$$

(vi) Factor of safety = $Q_u/P = 2178/1220 = 1.79 < 3.0$, hence the design is not safe against shear. Further, pressure intensity = $2178/4 = 544.5 \text{ kN/m}^2$

(vii) Design of footing resting on sand reinforced with Geogrid with the following arrangement:

$$N = 3, L_r = 3B \times 3B, U/B = S_v/B = 0.25$$

Geogrid–sand friction angle, $\phi_f = 22^\circ$
 Allowable tensile strength, $T_R = 20 \text{ kN/m}$
 LDR for geogrid = 1

The dimensionless quantities $J_{xz}, J_{yz}, I_{xz}, I_{yz}, M_{xz}, M_{yz}$, and A_{xz} and A_{yz} are obtained from non-dimensional charts, Figs. 4 and 5 and for $e/B=0.1$ and $i = 10^\circ$, for different layer levels as shown in Table 1. The values of $f_e T_D$ and T_f are calculated using Eqs. (2), (12), and (27), respectively.

The pressure ratio ' p_r ' for reinforced sand can be computed for a pressure intensity ' q_o ' for the unreinforced sand at a given settlement ' S '. For $e/B = 0.1$ and $I = 10^\circ$ the reduction factor due to

eccentricity and inclination of the applied load to be multiplied in the frictional force is given below. Let us determine the pressure ratio p_r for pressure intensity $q_o = 285 \text{ kN/m}^2$ at settlement S . There will be eight independent cases when $N = 3$, each giving a value of p_r . However, the critical value of p_r will be the minimum. In this example, case 3 and 4 are illustrated as follows:

$$R_{fe} = 1 - 2e/B = 1 - 2 \times 0.1 = 0.8$$

$$R_{fi} = 1 - i/\phi = 1 - 9.93/35 = 0.72$$

$$R_f = R_{fe} \times R_{fi} = 0.8 \times 0.72 = 0.58$$

Case 3: First layer fails in pull-out, while the rest fail in breaking

$$r_1 \times 5.387 \times 285 \times (p_r - 1)$$

$$\leq (0.823 \times 285 \times P_r + 719.28) \times 0.58$$

$$r_2 \times 3.724 \times 285 \times (p_r - 1) \leq 240$$

$$r_3 \times 2.698 \times 285 \times (p_r - 1) \leq 240$$

$$r_1 + r_2 + r_3 = 1$$

From, which, $p_r = 1.767$

Case 4: Second layer fails in pull-out, while the others fail in breaking

$$r_1 \times 5.387 \times 285 \times (p_r - 1) \leq 240$$

$$r_2 \times 3.724 \times 285 \times (p_r - 1)$$

$$\leq (0.993 \times 285 \times p_r + 719.57) \times 0.58$$

$$r_3 \times 2.698 \times 285 \times (p_r - 1) \leq 240$$

$$r_1 + r_2 + r_3 = 1$$

From, which, $p_r = 2.009$

Values of p_r for all eight cases are given in Table 2 for $q_o = 285 \text{ kN/m}^2$

As can be seen from Table 2, the critical value of $p_r = 1.417$, from case 2, in which all reinforcement layers fail in breaking for $q_o = 285 \text{ kN/m}^2$. But

$$Q = p_r \times q_o = 1.417 \times 285 = 403.8\text{kN/m}^2$$

$$Q \approx 404\text{kN/m}^2$$

Also, the pressure ratio has been obtained for pressure intensity $q_o=Q_u=545 \text{ kN/m}^2$, where, $p_r = 1.218$ (case 2)

$$\text{But } p_r = q/q_o$$

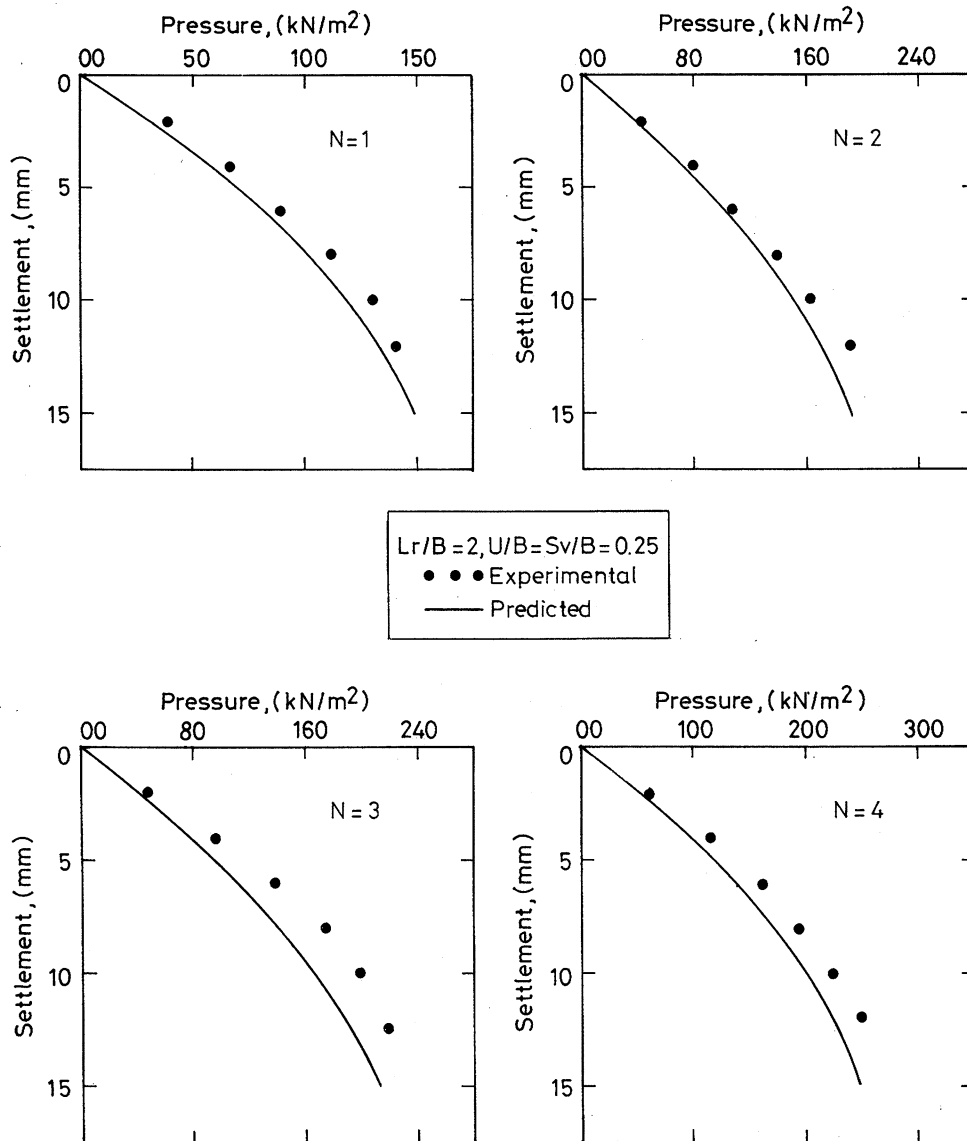


Fig. 8 Comparison of predicted and experimental pressure versus settlement curves for square footing on sand reinforced with Tensar SS20 geogrid, $e/B = 0.1$, $i = 10^\circ$, $L/B = 2$

$$q_r = p_r \times q_u = 1.218 \times 545 = 663.81 \text{ kN/m}^2$$

$$q_r \approx 664 \text{ kN/m}^2$$

Using Eq. (28), the ultimate bearing capacity of reinforced sand is given as:

$$q_{ur} = q_r + \gamma D_R N_q \times R_{iq} \times R_{eq} = 663.81$$

$$+ (15 \times 0.75 \times 2 \times 40 \times 0.8 \times 0.79)$$

$$= 663.81 + 568.8 = 1232.61 \text{ kN/m}^2$$

$$q_{ur} \approx 1233 \text{ kN/m}^2$$

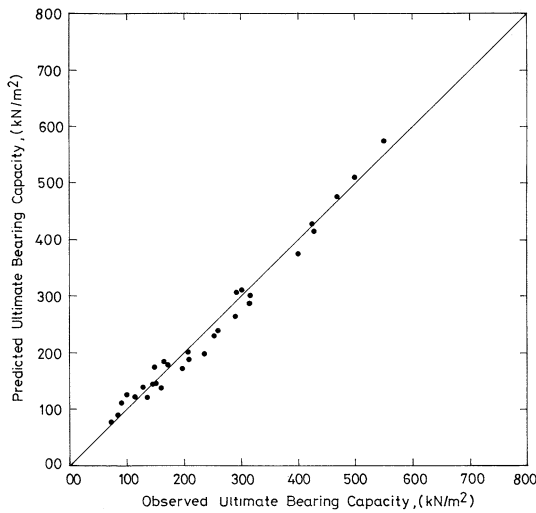


Fig. 9 Comparison of observed and predicted values of settlement of footings subjected to eccentric-inclined load, on sand reinforced with Tensar SS20 geogrid

But $Q_{ur} = q_{ur} \times A = 4932 \text{ kN/m}^2$ $FS = Q_{ur} / P = 4932 / 1220 = 4.04$ $FS = 4.04 > 3$ hence safe against shear failure.

Conclusions

In this investigation, the method of analysis presented by Binquet and Lee (1975a, b) and Kumar and Saran (2003b), for isolated strip footings has been extended to eccentrically and obliquely loaded square and rectangular footings on reinforced sand. Experimental results match very well with the proposed analysis. The computation of normal force on the reinforcement area and the estimation of interfacial frictional resistance at different layer levels are two essential steps in the computation of pressure ratio. The process has been simplified by presenting suitable charts in non-dimensional form that can be directly used for the same purpose. An approximate method has been proposed for the determination of ultimate bearing capacity of reinforced soil. Thus, the square and rectangular footings subjected to eccentric and inclined loads can be designed satisfying both shear failure and settlement criteria. The present analysis requires the pressure-settlement values of unreinforced soil as pre-requisite, which can be obtained using any method

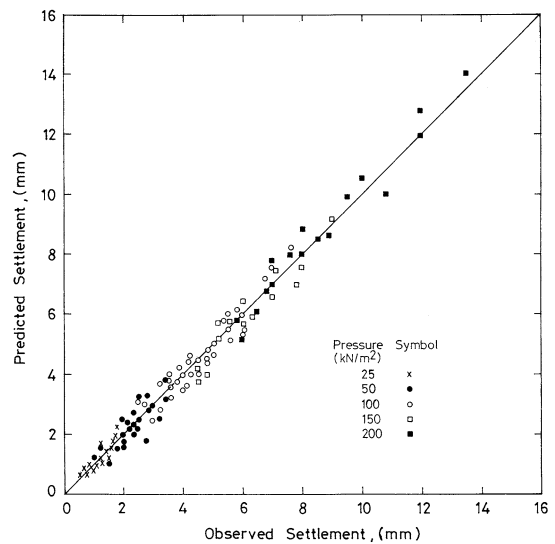


Fig. 10 Comparison of experimental and predicted values of ultimate bearing capacity of footings subjected to eccentric-inclined load on sand reinforced with Tensar SS20 geogrid

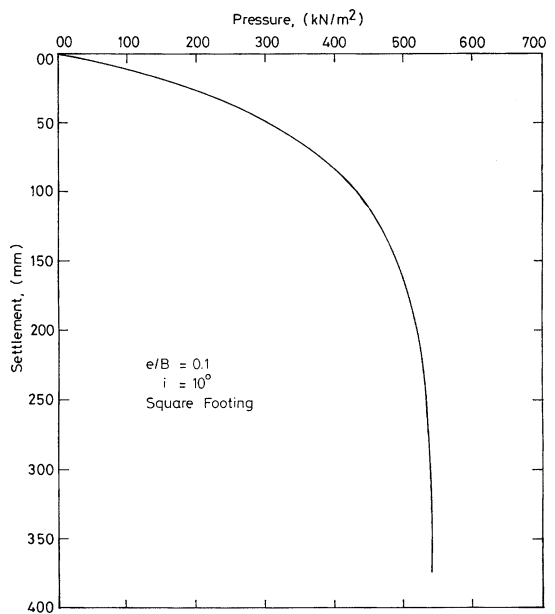


Fig. 11 Pressure versus settlement curve for square footing subjected to eccentric-inclined load, resting on sand (Design example)

available in literature. In the proposed analysis, a method suggested by Agrawal (1986) and Saran and Agrawal (1991) has been used to draw pressure settlement characteristics of eccentrically and obliquely loaded footings on unreinforced

Table 1 Calculation of forces for determination of pressure ratio, p_r

Z/B	$J_{xz}+J_{yz}$	$I_{xz}+I_{yz}$	$M_{xz}+M_{yz}$	$A_{xz}+A_{yz}$	f_e	T_D (kN)	T_f (kN)	T_{RF} (kN)
0.25	1.652	1.221	0.309	12.00	0.333	5.387 $q_o (P_r-1)$	0.823 $q_o P_r + 719.28$	240
0.50	1.438	1.014	0.472	11.40	0.263	3.724 $q_o (P_r-1)$	0.993 $q_o P_r + 719.57$	240
0.75	1.285	0.814	0.522	10.80	0.192	2.698 $q_o (P_r-1)$	0.802 $q_o P_r + 622.08$	240

Table 2 Pressure ratio (p_r) values for all cases

Case No.	p_r	Reinforcement failure mechanisms
1	2.961	All layers fail in pull-out
2	1.417	All layers fail in tension
3	1.767	1st layer fails in pull-out, others fail in tension
4	2.009	2nd layer fails in pull-out, others fail in tension
5	2.086	3rd layers fails in pull-out, others fail in tension
6	2.507	1st & 2nd layers fail in pull-out, other fails in tension
7	3.000	3rd & 4th layers fail in pull-out, other fails in tension
8	2.606	1st & 3rd layers fail in pull-out, other fails in tension

soil. Therefore, the limitations of the method used will also be incorporated in the analysis.

References

- Adams MT, Collin JG (1997) Large model spread footing load tests on geosynthetic reinforced soil foundations. *J Geotech Geoenviron Eng ASCE* 123(1):66–72
- Agrawal RK (1986) Behaviour of Shallow foundations subjected to eccentric inclined loads. Ph D thesis, University of Roorkee, Roorkee (India)
- Akinmusuru JO, Akinbolade JA (1981) Stability of loaded footings on reinforced soil. *J Geotech Eng Div ASCE* 107(GT6):819–827
- Al-Smadi MM (1998) Behavior of ring foundations on reinforced soil. PhD thesis, University of Roorkee, Roorkee (India)
- Binquet J, Lee KL (1975a) Bearing capacity tests on reinforced earth slabs. *J Geotech Eng Div ASCE* 101(GT 12):1241–1255
- Binquet J, Lee KL (1975b) Bearing capacity analysis of reinforced earth slabs. *J Geotech Eng Div ASCE* 101(GT 12):1257–1276
- Das BM, Larbi-Cherif S (1983) Bearing capacity of two closely spaced shallow foundations on sand. *Soils and foundations. Jap Soc Soil Mech Found End* 23(1):1–7
- Dixit RK, Mandal JN (1993) Bearing capacity of geosynthetic reinforced soil using variational method. *Geotext Geomembr* 12:543–566
- Fragaszy RJ, Lawton E (1984) Bearing capacity of reinforced sand subgrade. *J Geotech Eng Div ASCE* 110(10):1500–1507
- Guido VA, Chang DK, Sweeney MA (1986) Comparison of geogrid and geotextile reinforced earth slabs. *Can Geotech J* 23:435–440
- Huang CC, Tatsuoka F (1990) Bearing capacity of reinforced horizontal sandy ground. *Geotext Geomembr* 9:51–80
- Khing KH, Das BM, Puri VK, Cook EE, Yen SC (1993) The bearing capacity of strip foundation on geogrid reinforced sand. *Geotext Geomembr* 12:351–361
- Khing KH, Das BM, Puri VK, Yen SC, Cook EE (1994) Foundation on strong sand underlain by weak clay with geogrid at the interface. *Geotext Geomembr* 13:199–206
- Kumar (1997) Interaction of footings resting on reinforced earth slab. PhD thesis, University of Roorkee, Roorkee (India)
- Kumar S (2002) Behaviour of eccentrically and obliquely loaded footings on reinforced earth slab. PhD thesis, IIT Roorkee, Roorkee (India)
- Kumar A, Saran S (2001) Isolated strip footing on reinforced sand. *Geotech Eng J, Bangkok, Thailand, SEAGS* 32:177–189
- Kumar A, Saran S (2003a) Closely spaced footings on geogrid reinforced soil. *J Geotech Geoenviron Eng ASCE, ASCE* 129(7):660–664
- Kumar A, Saran S (2003b) Bearing capacity of rectangular footing on reinforced soil. *J Geotech Geol Eng Kluwer Acad Publ, The Netherlands* 21(3):201–224
- Kumar A, Saran S (2003c) Closely spaced strip footings on reinforced sand. *Geotech Eng J, Bangkok, Thailand, SEAGS, December* 34(3):177–189
- Kumar A, Saran S (2004) Closely spaced rectangular footing on reinforced soil. *J Geotech Geol Eng Kluwer Acad Publ, The Netherlands* 22:497–524
- Kumar A, Walia BS, Saran S (2005) Pressure settlement characteristics of rectangular footings on reinforced soil. *J Geotech Geol Eng* 23:469–481. Springer Science and Business Media, The Netherlands
- Murthy BRS, Sridharan A, Singh HR (1993) Analysis of reinforced soil beds. *Indian Geotech J* 23(4):447–458

- Omar MT, Das BM, Yen SC, Puri VK, Cook EE (1993a) Ultimate bearing capacity of rectangular foundations on geogrid-reinforced sand. *Geotech Test J ASTM* 16(2):246–252
- Omar MT, Das BM, Yen SC, Puri VK, Cook EE (1993b) Ultimate bearing capacity of shallow foundations on sand with geogrid-reinforcement, *Can Geotech J* 30(3):545–549
- Omar MT, Das BM, Puri VK, Yen SC, Cook EE (1994) Bearing capacity of foundations on geogrid-reinforced sand. 13th International Conference on SMFE, New Delhi, pp 1279–1282
- Poulos HG, Davis EH (1974) *Elastic solutions for soil and rock mechanics*. John Wiley and Sons. Inc., New York
- Saran S, Agrawal RK (1991) Bearing capacity of eccentrically obliquely loaded footing. *J Geotech Eng ASCE* 117(11):1669–1690
- Singh HR (1988) Bearing capacity of reinforced soil beds. PhD thesis, II Sc Bangalore (India)
- Yetimoglu T, Wu JH, Saglamer A (1994) Bearing capacity of rectangular footings on geogrid reinforced sand. *J Geotech Eng ASCE* 120(12):2083–2099
- Yoo C (2001) Laboratory investigation of bearing capacity behaviour of strip footing on geogrid-reinforced sand slope. *Geotext Geomembr* 19:279–298